Spatio-temporal dynamics of surface melting over Antarctica using OSCAT and QuikSCAT scatterometer data (2001–2014)

Rajashree V. Bothale*, P. V. N. Rao, C. B. S. Dutt, V. K. Dadhwal and Devesh Maurya

National Remote Sensing Centre (ISRO), Hyderabad 500 037, India

In this article, spatio-temporal dynamics of snowmelt in Antarctica from 2001 to 2014 using OSCAT and QuikSCAT scatterometer data is presented. Melting over Antarctic ice sheet can influence shelf dynamics and stability. Here, we have utilized the sensitivity of scatterometer data to detect the presence of liquid water in the snow caused due to melt conditions. After analysing decadal data, a spatial and temporal variation in the average backscatter coefficient was observed over the shelf areas. An adaptive threshold-based classification using austral winter mean and standard deviation of HH polarization is used which takes into account the spatial and temporal variability in backscatter from snow/ice. Significant spatio-temporal variability in melt area, duration and melt index was observed. Around 9.5% of the continent experienced melt over the study period. Larsen C and George VI shelves had maximum melt duration. The high correlation between melt duration obtained from satellite data and the positive degree day validates the efficacy of the melt algorithm used in the analysis and sensitivity of OSCAT data in detecting presence of water due to melt. There is seasonal and spatial variation in melt onset. Based on MI, 2004–05 was the warmest summer over the continent with 2011–12 being the coldest summer. Consistent and intensive melting was observed over Amery, Larsen C, George VI, Lazarev and Fimbul shelves. Melting of sporadic nature was observed over Ronne–Filchner, Ross and Riiser–Larsen shelves. The East Antarctic shelves experienced large melt during the study period. This article presents the suitability of OSCAT in melt identification and status of melt over the continent.

Keywords: Ice shelves, scatterometer data, spatio-temporal dynamics, snowmelt.

ANTARCTICA ice sheets play an important role in influencing the climate system. An increase in the western continent melt activity has been observed in the recent past, which has resulted in the breaking of the ice shelf from the continent (www.antarcticglaciers.org). The continent has many ice shelves at the fringes which respond to exposure to the warming air above and the warming polar ocean below. Global climate change has a great impact on the ice shelves, because they are sensitive to changes in air and ocean temperature or circulation near Antarctica[1]. Increased atmospheric temperatures lead to surface melting and ponding on the ice surface[2]. Catastrophic ice-shelf collapse tends to occur after a relatively warm summer season, with increased surface melting[2]. Antarctic ice sheet surface melting can regionally influence ice-shelf stability, mass balance and glacier dynamics, in addition to modulating near-surface physical and chemical properties over wide areas[3].

In situ measurements also indicate melting conditions in Antarctica, but to get the spatial distribution of melt, researchers have used active as well as passive microwave data for identification and mapping of surface melt over the continent[4–7]. Studies based on passive microwave radiometry have used brightness temperature data obtained at different channels[8–12]. Estimation of the extent, onset date, end date and duration of snowmelt in Antarctica from 1978 to 2004 was done using scanning multichannel microwave radiometer (SMMR) and special sensor microwave imager (SSM/I) data. The results indicate periodic melting over Amery ice shelf and occasional melting over Ross Ice shelf[5].

Extensive work has been done in the past using scatterometer data to identify snowmelt[3,4,6,13–18]. Owing to the similarity between Quik Scatterometer (QuikSCAT) and Oceansat Scatterometer (OSCAT), OSCAT is viewed as a continuity mission for QuikSCAT[17]. An empirical, grid cell-specific thresholding method using QuikSCAT data (2000–2004) has been used to identify melt/freeze over Eurasian Arctic ice masses[19]. QuikSCAT data for the period 2000–2009 with wavelet detection algorithm have been used to identify melt over Antarctica and it has been suggested that the ability to classify melting based on relative persistence is a critical aspect of the wavelet-based algorithm[20]. QuikSCAT data have been used to derive Melt Index (MI) and observed correlation between MI variation and rift propagation over Amery shelf[17].

*For correspondence. (e-mail: rbothale@gmail.com)

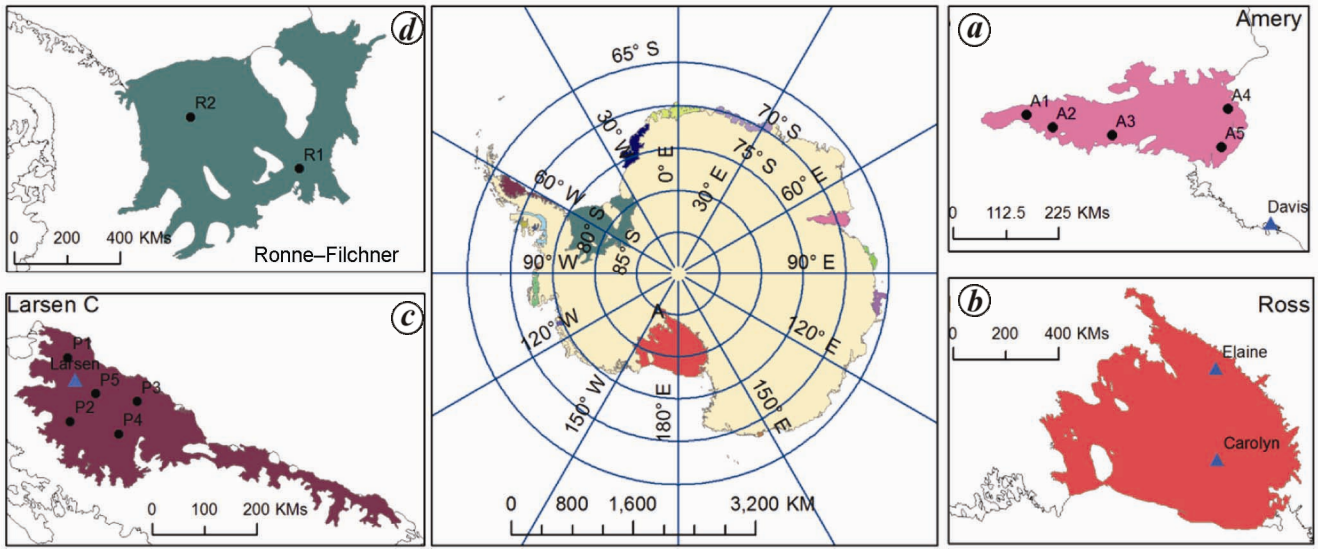

Figure 1. Location of AWS stations (triangles) and test sites (black circles) on (***a***) Amery, (***b***) Ross, (***c***) Larsen C and (***d***) Ronne shelves on Antarctica.

The present article is based on a study of the spatio-temporal dynamics of surface melting along with the melt duration over Antarctica and an update on the previous results of mapping by analysing scatterometer data available up to February 2014. The relation between MI and ENSO indices is also discussed.

Data used and methodology

OSCAT and QuikSCAT enhanced resolution images and time series of backscatter coefficient (σ^0)

The study utilizes data from SeaWinds on-board 'QuikSCAT' (2001–2009) and OSCAT on-board 'Oceansat-2' (2009–2014), which are K_u band (13.6 GHz) active microwave scatterometers and operate in dual-polarization mode of HH and VV providing daily coverage of the polar regions. Enhanced resolution daily images at 2.25 km resolution for both HH and VV polarization were downloaded from the website http://www.scp.byu.edu for the period January 2001 to February 2014. Antarctica has many shelves all around the periphery, out of which the four major ones are shown in Figure 1. To understand the temperature and melt analogy, data from automated weather stations (AWS) on Larsen C, Ross and near Amery (triangles in Figure 1) were used in the study. For detailed analysis of backscatter response, few test sites were marked on Amery, Larsen C and Ronne–Filchner shelves (black circles in Figure 1).

To understand the behaviour of OSCAT response to different snow/ice conditions, time series of σ^0 was plotted for the test sites on Amery (Figure 2 *a*), Larsen C (Figure 2 *b*) and Ronne–Filchner shelves (Figure 2 *c*) and for AWS sites on Ross shelf (Figure 2 *d*). From Figure 2 *a* and *b* it is clear that there is a steep reduction in σ^0 values (of the order of 15 dB or more) during austral summer compared to the preceding winter mean. Normalized radar backscatter is sensitive to the water content of snow. With increase in the liquid water content of snow, there is a sudden decrease in the backscatter values from the radar. Sensitivity of the backscatter to snow wetness depends upon the microwave frequency. A change in wetness from 0% to 1.26% results in a drop in level of 1 dB at 1 GHz, but as the frequency increases, the difference between wet and dry curve increases to a maximum at 35.6 GHz (ref. 21). This is the basis of melt detection. Snow layer wetness and roughness of the snow cover affect the backscattering coefficient of wet snow because major contribution of backscatter is caused by the air–snow interface[22]. As reflectivity of wet snow is larger than that of dry snow by a fraction of 6, the backscatter model for wet snow is constructed by treating the upper snow boundary as a rough surface[23]. Surface scattering dominates over volume scattering in the case of wet snow. The presence of liquid water in snow volume causes a drastic increase in the dielectric loss factor of the layer, which increases the absorption coefficient and reduces the penetration depth[15,23]. Identification of onset of melt is possible through temporal variations in the backscatter. After studying the time series for HH and VV polarization along with polarization ratio ($\sigma^0_{VV} - \sigma^0_{HH}$) and polarization index ($\sigma^0_{VV} - \sigma^0_{HH}/\sigma^0_{VV} + \sigma^0_{HH}$), it was decided to use σ^0_{HH} due to greater dynamic range and sensitivity of HH polarization to liquid water content[4,15].

It is also clear from Figure 2 *a* and *b* that the backscatter response varies spatially over Amery and Larsen C shelves. This limits the use of fixed threshold for

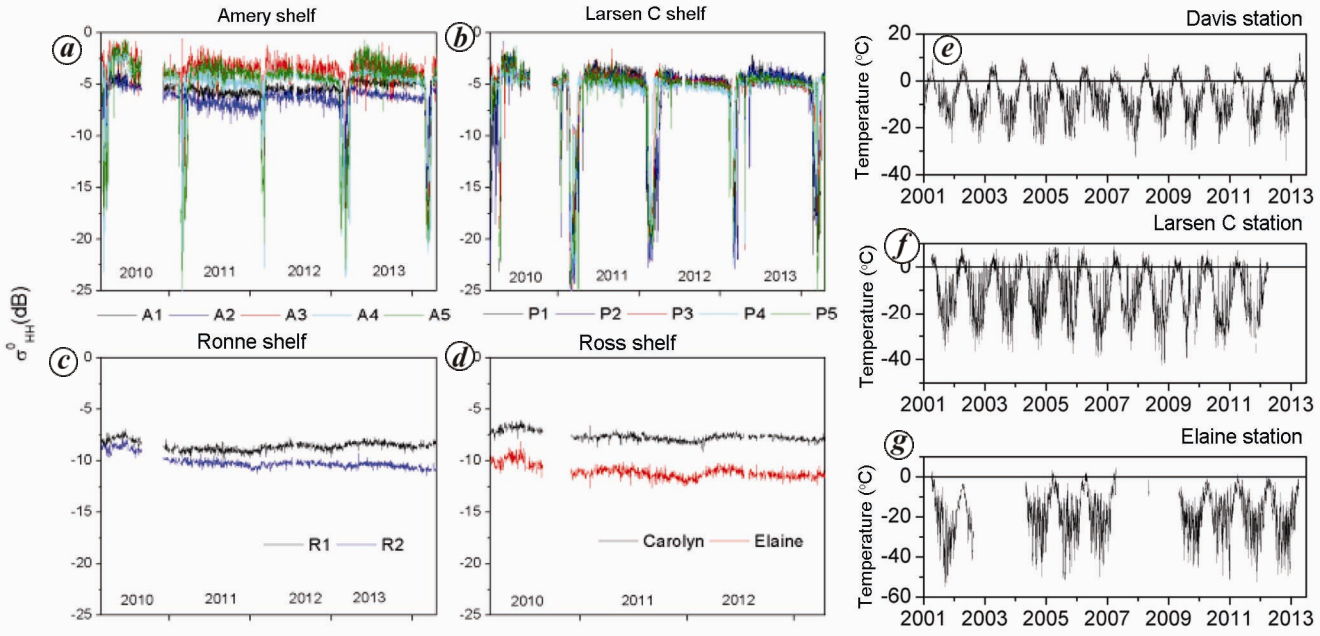

Figure 2. ***a*–*d***, Time series of σ^0_{HH} (dB) for January 2010 to February 2014 over (***a***) Amery, (***b***) Larsen C, (***c***) Ronne and (***d***) Ross shelves using OSCAT data. Location of the points are shown in Figure 1. ***e*–*g***, Time series of temperature from 2001 to 2013 over (***e***) Davis, (***f***) Larsen C and (***g***) Elaine stations.

detection of melt[15,24]. Backscatter response from test sites over Ronne–Filchner shelf (Figure 2 *c*) and AWS stations of Carolyn and Elaine stations of Ross shelf (Figure 2 *d*) indicate almost no reduction in backscatter response over the observed years, indicating practically no melt conditions over the shelf.

Temperature data from AWS

The data pertaining to Davis station (–68.576°, 77.967°; Figure 1) which is the nearest AWS station to Amery ice shelf, were obtained from the Australian Antarctica Division (http://data.aad.gov.au/aadc) for the period 2001 to 2014. AWS data for Ross ice shelf (Elaine station, –83.094° lat. and 174.285° long.) and Larsen shelf (Larsen station, –67.02° lat. and –61.56° long.) were obtained from the University of Wisconsin (UW), Madison, USA for the period of 2001–2013. Time series of temperature data at different stations correlate well with the σ^0_{HH} time series as shown in Figure 2 *a* and *b* with reduction in σ^0_{HH} associated with above zero temperature and no reduction in σ^0_{HH} when temperature remains below freezing point (Figure 2 *e*–*g*).

Melt/freeze detection from time series of backscatter coefficient σ^0_{HH}

Based on the austral winter mean (σ^0_{HHMW}), standard deviation (σ^0_{HHSDW}) and drop in σ^0 for austral summer (σ^0_{HHDS}) (Table 1), considering the spatio-temporal variability in σ^0_{HH}, an adaptive threshold based classification methodology is used for identification of melt/freeze over the continent.

Table 1. Winter mean, standard deviation and drop in backscatter during summer for Amery, Larsen and Ross shelf sites

Shelf site	Average backscatter coefficient (dB)			
Amery	2010	2011	2012	2013
σ^0_{HHMW}	–4.12	–4.91	–4.75	–4.46
σ^0_{HHSDW}	0.63	0.57	0.37	0.58
σ^0_{HHDS}	13.72	10.69	15.53	22.19
Larsen	2010	2011	2012	2013
σ^0_{HHMW}	–4.42	–4.35	–4.77	–7.35
σ^0_{HHSDW}	0.42	0.56	0.25	0.37
σ^0_{HHDS}	6.56	10.18	8.79	7.35
Ross	2010	2011	2012	2013
σ^0_{HHMW}	–8.79	–9.58	–9.44	–9.55
σ^0_{HHSDW}	0.31	0.31	0.31	0.31
σ^0_{HHDS}	1.86	1.11	0.97	1.32

A melt grid (MG) is a grid which satisfies the following criteria

$$\text{MG} = \text{True, if}\ \sigma^0_{HHn} < (\sigma_{HHMW} - 2 * \sigma^0_{HHSD_{max}}), \quad (1)$$

$$\text{MG} = \text{False, if}\ \sigma^0_{HHn} \geq (\sigma_{HHMW} - 2 * \sigma^0_{HHSD_{max}}), \quad (2)$$

where σ^0_{HHn} is the HH backscatter for the *n*th day and $\sigma^0_{HHSDW_{max}}$ is the maximum standard deviation of austral winter HH backscatter for the study area. An adaptive threshold helps in capturing the backscatter characteristics of an individual grid due to its location in the ice-shelf area in comparison to other methods where fixed

threshold was used, e.g. (3.5 and 5 dB)[19] or (2.0 and 3.0 dB)[25]. For the year 2009–10, where analysis included calculation of austral winter mean from QuikSCAT and melt detection from OSCAT, an additional offset of 0.5 dB was deducted from the adaptive threshold to get the melt pixel. At the calibration sites the offset between both the sensors was found to be 0.25 dB (ref. 26). To identify the onset of melt, the first of two consecutive days where melt had occurred was marked as the onset of melt. Melt duration was calculated by adding days when a particular grid was under melt based on the above criteria.

Melt index and relation with different predictors: To study inter-annual variability in melt, the melt index[8] is used, which is defined as follows

$$\mathrm{MI} = \sum_{i=1}^{N} A \cdot mdi, \tag{3}$$

where A is the size of one grid, mdi the number of melt days (MD) for the grid i and N is the total number of grids. The summation of MI is done for the austral summer between November and February.

In order to understand the melt behaviour, a degree day concept is used[27]. A positive degree day (PDD) assumes that for every 1°C above 0°C, a certain amount of melt will take place. PDD sum (PDDS) which is the sum of temperatures above 0°C is calculated for austral months over different study years for Davis and Larsen stations as follows

$$\mathrm{PDDS} = \sum_{j=1}^{N} T_j, \quad \forall T_j > 0. \tag{4}$$

Although surface snowmelt is not directly proportional to air temperature due to nonlinear interactions between components of the surface energy balance, the PDD approach gives robust empirical relationship between melt and air temperatures[6]. The connection between monthly average temperature (T_{mm}), PDD and PDDS is studied to understand the melt dynamics over the continent.

Results and discussion

Based on the variable threshold logic, daily data were analysed to identify melt grids over Antarctica.

Spatial variability in melt and duration

Figure 3 shows the average melt duration map generated for the period 2001–2014. Primarily, melt was observed over shelves, except for a small area near Ross. Melt was detected over the Transantarctic Mountains during January 2005, 875 km inland and 2000 m asl (refs 3, 10, 28). The observed maximum melt duration of 90 days, was divided into high (61–90), medium (31–60), low (3–31) and very low (<3) days. Spatial variability shows high and medium melt days over Antarctic Peninsula, mainly on Larsen C, George VI, Getiz and Bach shelves. Low melt is observed over Riiser–Larsen, Fimbul, Lazarev and Nickerson shelves. Amery shelf falls under medium and low melt duration. For two days very low melt was observed over Ross and Ronne shelves during the study period. Shakleton and West ice shelves also show high melt pattern similar to that of west Peninsula, indicating that the East Antarctic shelves are not immune from melting[17].

Year-to-year variation is observed in the frequency of melt duration and area over Antarctica (Figure 4). The continent had maximum melt of one day during 2010–11 and 2013–14. Around 9.5% of the continent experienced melt of one week or less according to the present analysis. Also, 0.32% of the continent had melt duration of 77 days and more. During the analysis period 1978–2004, 25% of the continent was reported under melt due to excessive melt occurring on Ross and Ronne shelves before 2000 (ref. 5). In another study[3], no clear trend was reported over the study period 1999–2009 using QuikSCAT data.

Figure 5 shows the melt behaviour of 16 major shelves. The shelves are important either due to their area or their location on the continent. Ross is the largest shelf and Getz is the smallest shelf whose results are presented here. Larsen and George VI shelves (30–120° W in Peninsula and Mary Byrd Land) show more number of days under melt. Larsen C has melt duration between 1 and 100 days, whereas for George VI it is 1 to 95 days. Wilkins shelf has melt duration of 40–100 days, whereas for Bach shelf it varies between 10 and 90 days, with more pixels observing melt between 50 and 90 days in Mary Byrd Land. Ronne–Filchner has a small area under melt duration of 2–3 days. The three major shelves, viz. Riiser–Larsen, Fimbul and Lazarev (30°W to 60°E in Dronning Maud Land) have almost similar melt duration pattern. Amery shelf, which is a major shelf (60–150°E), has the number of melt days as 60. Shakleton and West shelves in Wilkies land have melt duration of 10–70 days and the frequency pattern is also similar. Antarctica zone between 150°E and 120°W has Ross, Cook and Nickerson shelves with varying melt conditions. Cook and Nickerson shelves which form part of Marie Byrd Land have melt duration of 1–50 and 1–40 days. Ross shelf has melt duration of less than 10 days (2% of shelf area only) with majority of area experiencing average melt duration of 1 day during 2013–14. Trend in melt duration was calculated for major shelves using 2001–2014 data (Table 2). Significant trend is observed only over six shelves, majority of which lie in the Antarctic Peninsula.

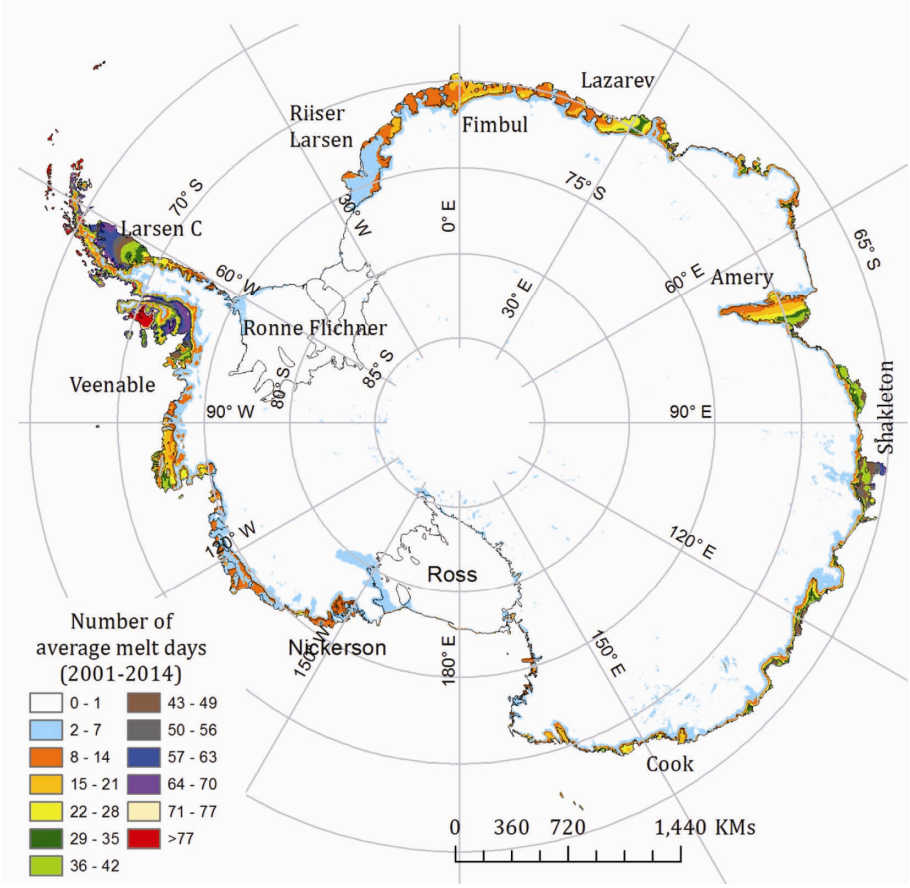

Figure 3. Spatial variability in average annual melt duration over Antarctica (2001–2014).

Table 2. Trend in melt duration over different shelves

Shelf	Trend	Significance*
Abbott	–0.74	0.443
Amery	–1.50	0.135
Bach	–2.74	**0.018**
Cook	–0.21	0.781
Dotson	0.10	0.829
Fimbul	–0.25	0.763
George VI	–2.73	**0.007**
Getz	–4.09	**0.004**
Larsen C	–3.30	**0.007**
Lazarev	–0.30	0.735
Nickerson	–0.08	0.903
Riiser–Larsen	–0.41	0.304
Ronne–Filchner	–0.14	**0.006**
Ross	–0.32	0.065
Shakleton	–1.40	0.052
Venable	–0.56	0.368
West	–1.37	0.153
Wilkins	–2.45	**0.016**

*Note: Significant trends at 95% are given in bold.

Temporal variation in melt onset

Spatio-temporal variations in melt onset (Figure 6 *a*) show year-to-year and spatial variability over the continent. Figure 6 *b* shows the melt onset days for amery shelf. There is year-to-year variability, as shown in Figure 6 *a* and *b*. During 2003–2006, the melt onset over Amery took place in the first and second fortnight of December. In 2013–15, the melt onset is observed during the first fortnight of January (minimum two days continuous melt).

To understand the seasonal cycle of surface melt over different shelves, daily melt extent values were averaged to get date-wise average melt extent. Table 3 shows the average peak melt date over major shelves.

Average date of occurrence of maximum melt depends upon the number of observation years used in the analysis. In a similar study for Amery shelf using data of 2009–2014, maximum melt was reported on 9 January[29].

Inter annual variability in melt

Time series of MT and MA are plotted in Figure 7, which shows large interannual variability in many parts of Antarctica. The Peninsula shelves had minimum melt index during 2013–14 indicating cold summer, whereas Amery shelf had warm summer in 2012–13 and 2013–14.

Austral summer of 2012–13 was warm for Riiser–Larsen, Fimbul and Lazarev in Dronning Maud Land.

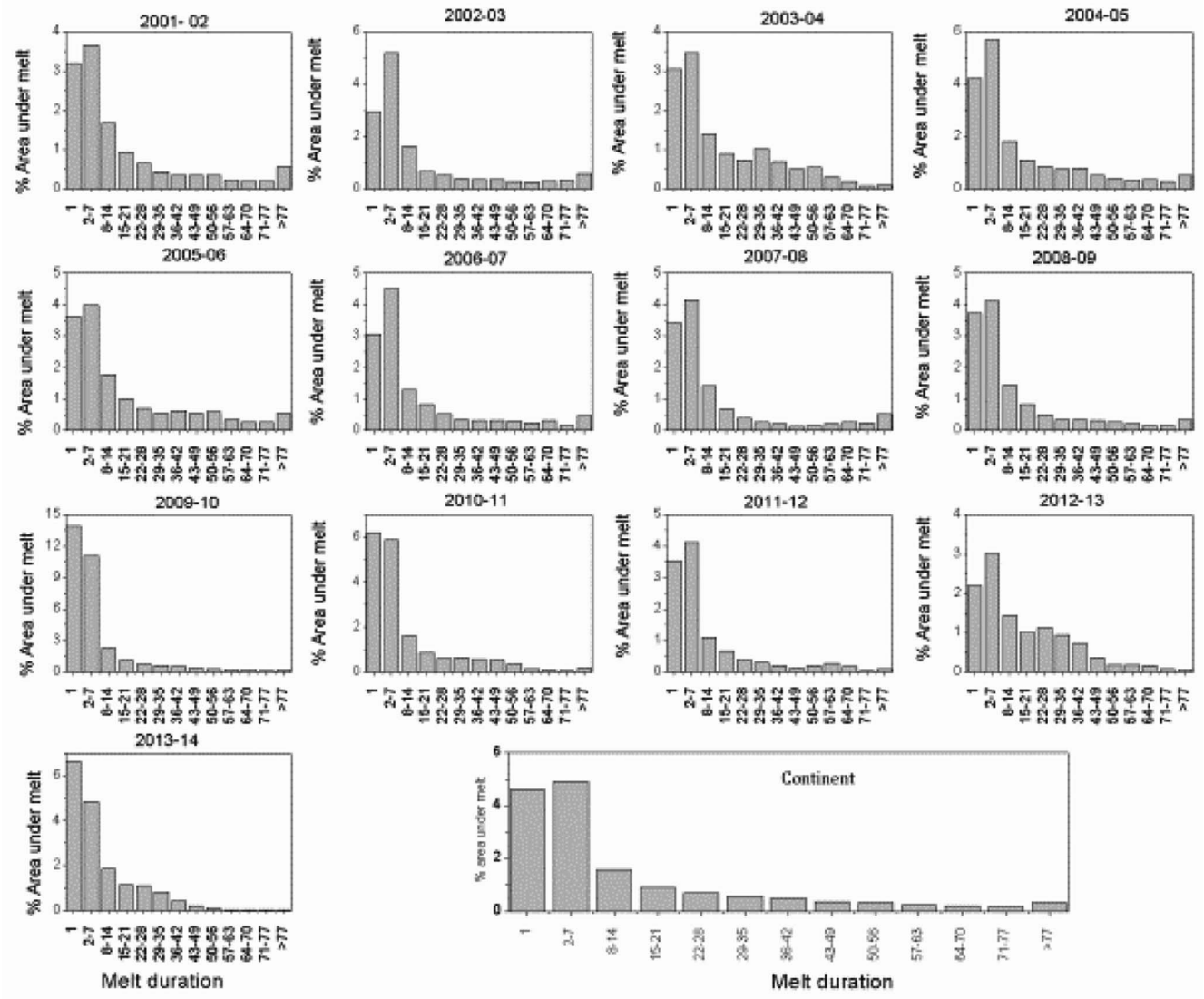

Figure 4. Frequency of melt grids with melt duration over Antarctica.

Table 3. Average peak melt date over different shelves

Shelf	Average date of maximum melt
Abbott	21 December
Amery	9 December
Bach	14 December
Cook	29 December
Dotson	22 December
Fimbul	19 December
GeorgeVI	14 December
Getz	13 December
LarsenC	15 December
Lazarev	23 December
Nickerson	5 January
Riiser–Larsen	12 January
Ronne–Filchner	13 January
Ross	14 January
Shakleton	10 December
Venable	12 November
West	7 December
Wilkins	12 November

The warmest summer was observed in 2004–05 and 2005–06, with 2011–12 observed as the coldest summer. An earlier study also showed no specific trend in melt volume[7]. Widespread melting was observed between 1989 and 1992 (ref. 30) and a 30-year minimum during austral summer of 2008–09 was also reported[31]. Taking the entire continent under consideration, Figure 8 shows the MI and MA scenario. The year 2004–05 was the hottest summer with maximum MI and 2011–12 was the coldest summer with lowest MI. Towards an objective analysis of interannual variability, no clear picture had emerged and the melt was not found to be consistent with circumpolar travelling wave[9].

Since melt index incorporates melt duration, there exists a high spatio-temporal correlation between MI and MD. Yet there are large areas where these two parameters are not correlated well, providing information about the diversity of melt process over the continent. The

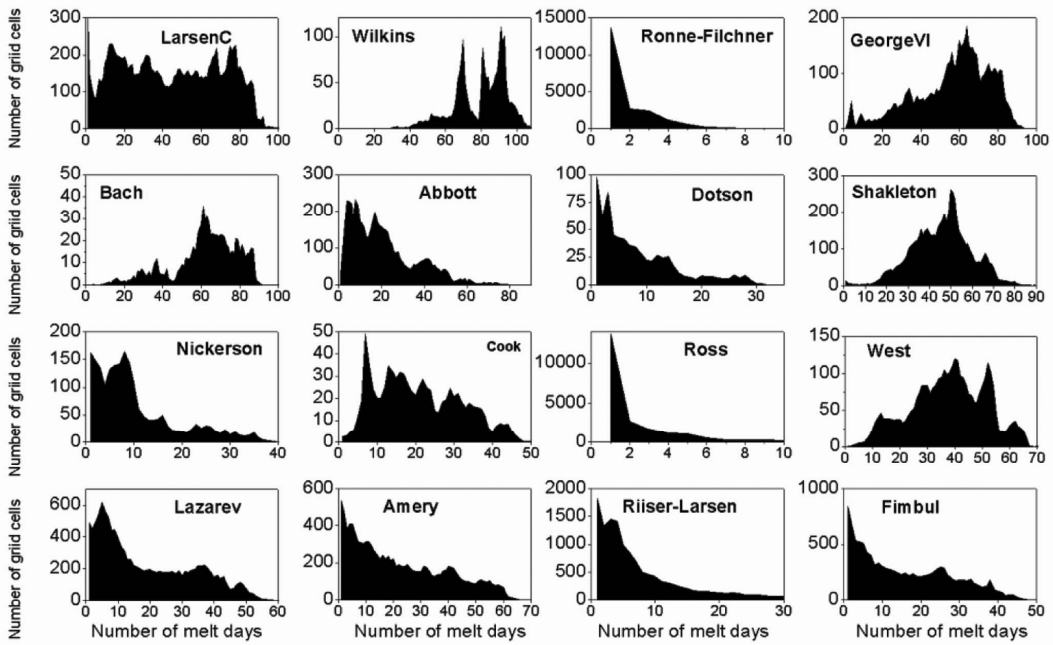

Figure 5. Shelf-wise variation in average number of melt days (2001–2014) for major shelves. Horizontal axis shows the number of melt days and vertical axis the number of grids in melt condition over the shelf.

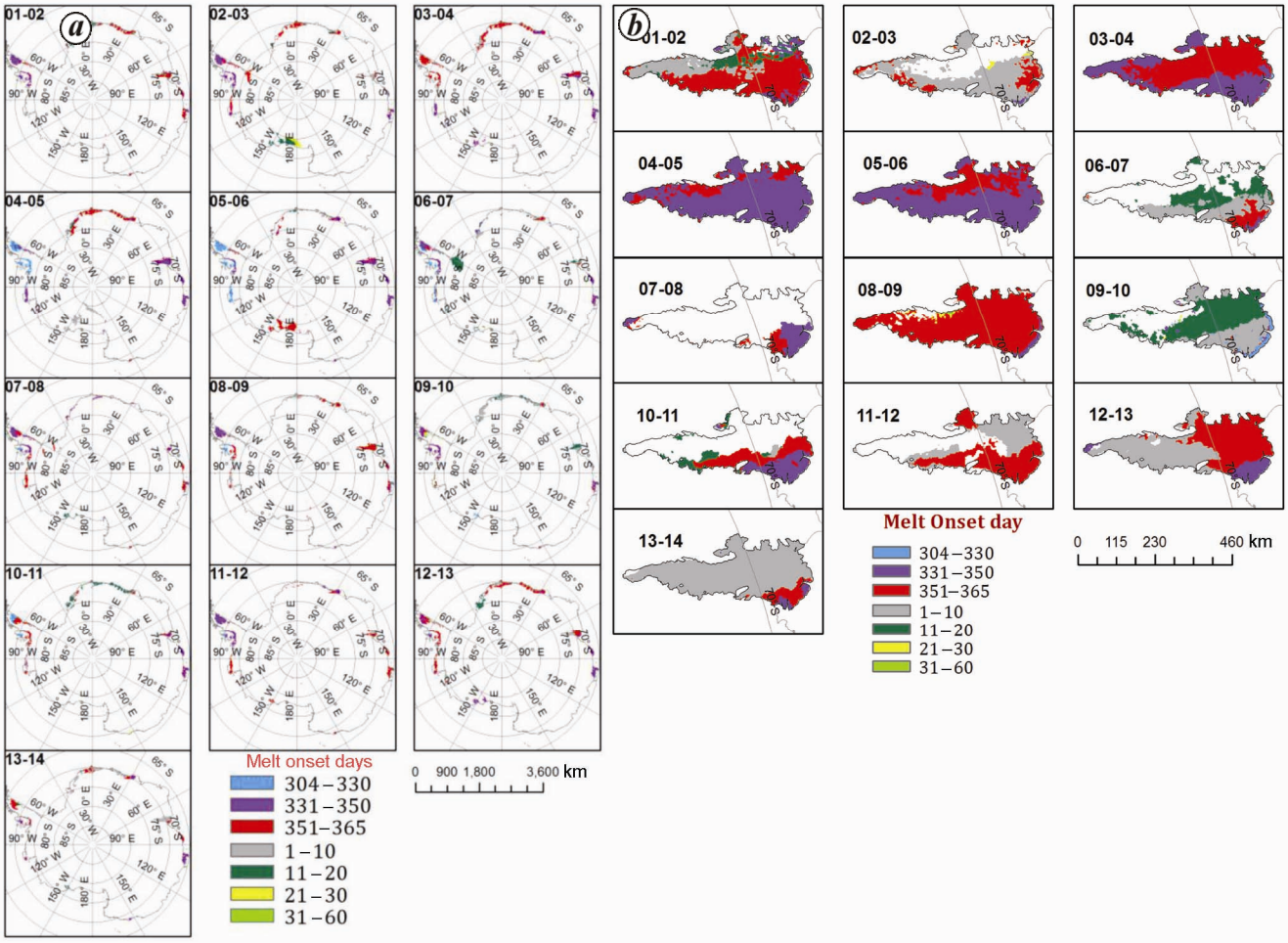

Figure 6. ***a***, Melt onset dates for Antarctica during 2001–2014. ***b***, Onset days for Amery shelf. The onset days are marked for the areas with observed melt for two days and more.

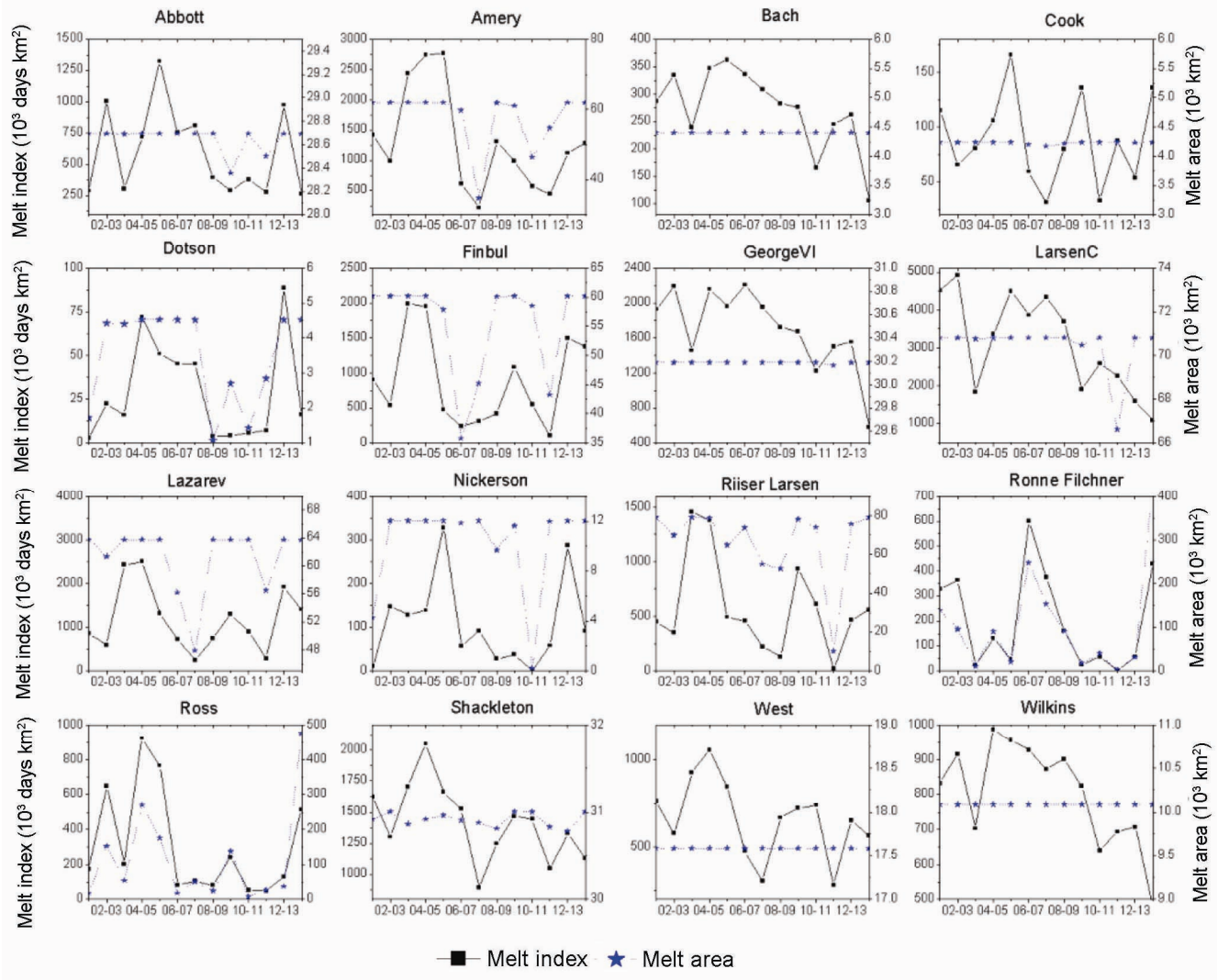

Figure 7. Interannual variability of melt area and melt index.

information provided by melt index depends upon the shelf area as well. For shelves like Antarctic Peninsula where surface area availability is low, the melt index will depend upon melt duration[3]. Over large shelves, the area available for melt is high, although shelves like Ross and Ronne undergo melting process for a short duration of time. High significant correlation between MI and MD was found over Ross, Riiser–Larsen, Larsen C, Shakelton, George VI and Abbott shelves.

As mentioned earlier, Figure 8 shows melt index and melt area for entire continent. Both MI and MA were highest in 2004–05 (ref. 17). The year 2005–06 saw a drop in MA, whereas MI still remained high. This indicates melt over small area, but with more duration[3]. In 2010–11, the continent had a large area under melt, but the duration was less, hence MI was less. For the austral summer of 2011–12, both melt area and duration were minimum, thereby reducing MI to an overall minimum as shown in Figure 8. In a study using data of 1980–1999, a decrease of 1.8% was reported which was consistent with mean January cooling of the continent[9]. It has been reported that melting extent and index have been decreasing over Antarctica, since 1987, although neither positive nor negative trend was observed from a sub-continental scale analysis[10]. In another study using data of 2000–2009, a strong relation was observed between melt index and intensity, but no clear trend has emerged over the years[3]. The melt index obtained from the present study was found to be in tune with other studies[3,31].

Temperature and melt correlations

There is interannual and spatial variability in T_{mm} and PDD over the continent. As the time series considered for the analysis is not too large, the correlation between T_{mm} and PDDS for Amery and Larsen shelves in Eastern and Western Antarctica respectively, was found using

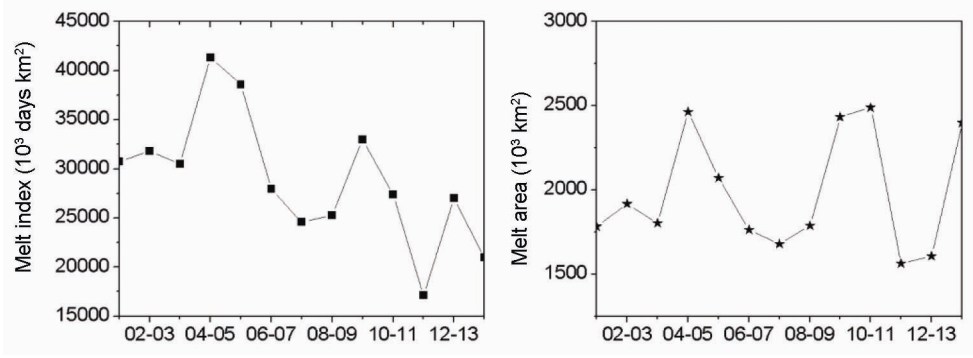

Figure 8. Melt index and melt area for the entire continent.

Table 4. Regression analysis statistics for Amery and Larsen shelves using mean austral month temperatures

Location	Amery	Larsen	Amery	Larsen	Amery	Larsen
Parameter	MI, T_{mm}		MI, PDDS		MD, PDD	
Regression	$MI = A*e^{B*T_{mm}}$		$MI = A + B*PDDS$		$MD = A + B*PDD$	
A	0.02325	0.14821	0.0346	0.0478	0.38843	6.438
B	0.48909	0.29207	0.0016	0.0031	0.883	0.859
R^2	0.72	0.68	0.64	0.50	0.716	0.81
P-value	0.062	0.03883	0.01298	0.00048	0.04869	0.0501

data from 2001 to 2014. A significant and reasonably good correlation is observed between PDDS and T_{mm} for Larsen ($PDDS = 24.09e^{0.6027}T_{mm}$ ($r^2 = 0.75$)) and Amery ($PDDS = 26.359e^{0.4026}T_{mm}$ ($r^2 = 0.81$)) stations respectively (Figure 9). The austral T_{mm} for Amery shelf varies between –4.00°C and 5.27°C with 71% of the time, temperature occurring above 0°C. The austral T_{mm} for Larsen C shelf varies between –6.34°C and 4.08°C with 50% of the time, temperature occurring above 0°C. These temperature values indicate warmer summer in Eastern Antarctica over Amery and relatively less warm summer over Antarctic Peninsula in Western Antarctica.

The relation between melt occurrence (MD and MI) and temperature was found by analysing mean monthly austral temperature (T_{mm}) and parameters like PDD and PDDS for Amery and Larsen shelves. Due to non-availability of temperature data and sporadic incidences of melt, temperature analysis could not be done for other shelves. A regression was developed between MI and T_{mm}, which shows that these two parameters are better correlated with non-linear regression and significant correlation exists (Figure 10 and Table 4). Although the correlation is high (0.72) for Amery, it is less significant. Melt tends to increase exponentially with increase in temperature. It is clear from Figure 10 that melt is introduced even when T_{mm} is negative. The melt in Antarctica is generally related to positive temperature. To understand the relation, MI was regressed with PDDS which is an indicator of the total amount of energy available for the melt. A high significant linear relation between MI and PDDS with r^2 of 0.64 and 0.50 was obtained in the analysis.

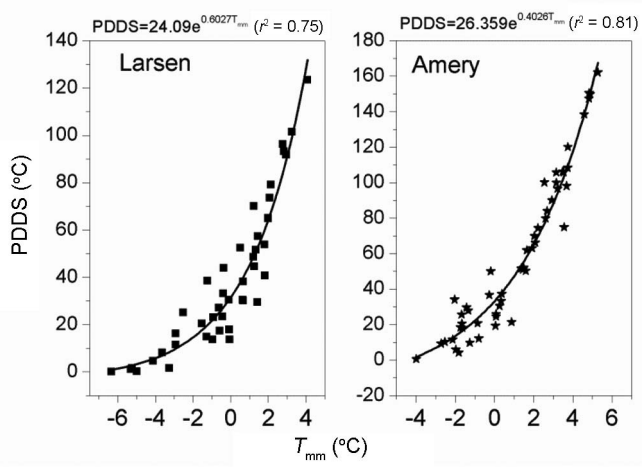

Figure 9. Correlation between positive degree day sum (PDDS) and mean monthly austral summer temperature (T_{mm}) for Larsen (West Antarctica) and Amery (East Antarctica) stations.

To understand the melt introduced at negative T_{mm}, the relation between MD and PDD was analysed, which shows a positive linear trend for Amery and Larsen shelves. The high correlation indicates the effectiveness of melt algorithm used in the analysis. Behaviour pattern of Amery and Larsen shelves is different as shown in Figure 10, where the dotted line is the perfect synergetic line. Majority of points in the lower half for Amery indicate lower surface temperature than air temperature. Temperature slightly above 0°C will increase PDD, but might not cause melt. In a similar analysis correlation of 0.859 was obtained between PDD and MD using

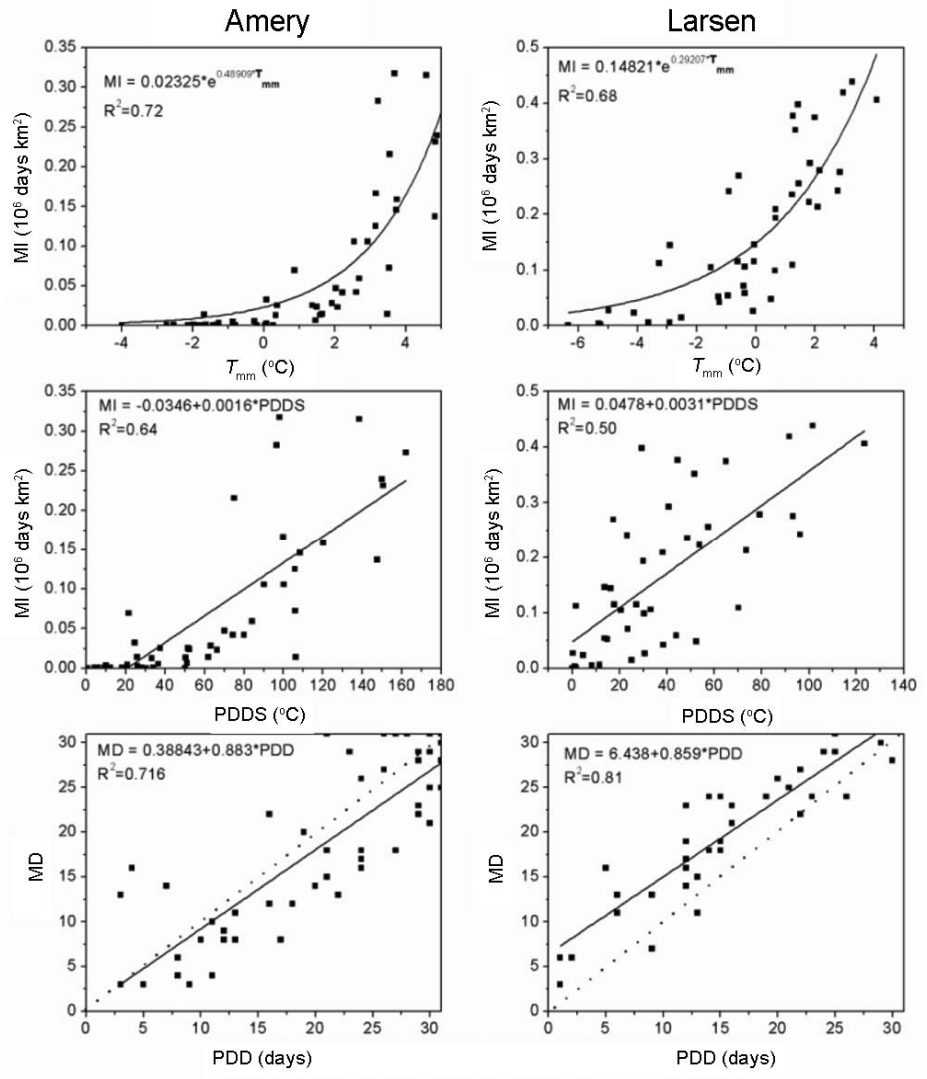

Figure 10. Relationship between melt index, mean monthly austral temperature, positive degree days, sum of positive degree days and melt days (using satellite data) over Amery and Larsen shelves.

QuikSCAT data[3]. Larsen had more number of melt days in comparison to PDD, indicating occurrence of melt even at sub-zero temperature. This might be due to availability of energy for melt or sensitivity of scatterometer to liquid water on the subsurface. Detailed analysis is needed in this regard. In spite of variations in the observations, we can conclude that a strong relation exists between MD and PDD over the study area. The equations can be used to generate PDD and PDDS maps using spatially available temperature data[6].

Melt index and ENSO indices

To understand the impact of large-scale environment variables, correlation was found between MI and oceanic nino index (ONI), Southern Oscillation index (SOI), multivariate ENSO index (MEI) and southern hemisphere annular mode (SAM) obtained from the website, http://www.esrl.noaa.gov/psd/data/climateindices/list/ and http://www.lasg.ac.cn/staff/ljp/data-NAM-SAM-NAO/SAM(AAO).htm#. The monthly values pertaining to June–August (JJA), October–December (OND) and December (D) were used. We found shelf-wise correlation between MI and ONI (JJA, $r = 0.56$), MI and SOI (OND, $r = -0.67$), MI and MEI (OND, $r = 0.47$) and MI and SAM (D, $r = -0.73$). To obtain statistical significance of the trends calculated for different parameters, a two-tailed *T*-test was carried out at 5% significance level. In trend analysis a null hypothesis assumes that nothing has happened or changed. To reject a null hypothesis, a result has to be identified as statistically significant. To determine the significance of the result, probability value (*P*-value) was calculated which should be less than the significance level. If the *P*-value is < 0.05, there is a significant trend in the observed time series. In the present analysis, *P* was more than 0.05 and hence the trends were insignificant.

The results show that MI is correlated with negative anomaly of December SAM. Although the results are not significant, they are consistent with those obtained by others[6], where October, November, December, January (ONDJ)-averaged SAM index correlated well with melt index. Various studies done in the past have shown the relationship between indices and the melt[17,32].

Summary and conclusions

In the present study, melt extent, duration and melt index were calculated using scatterometer data from QuikSCAT (SeaWinds) and Oceansat-2 (OSCAT) for the period 2001–14 using adaptive threshold method which utilizes austral mean and standard deviation. Spatio-temporal variability in melt pattern was observed (Figures 3 and 4) with maximum one-day melt during 2009–10, 2010–11 and 2013–2014, specially over Ross and Ronne shelves. Melt was observed mostly over the ice shelves than the other part of the continent. During the study period, around 9.5% of the continent was found to be under melt of one week or less duration. Shelf-wise variation in melt days was observed with higher melt duration (~100 days) in West Antarctica but with significant negative trend. Melt pattern in Drauning Maud land was similar for Riiser–Larsen, Fimbul and Lazarev. Shelf-to-shelf and year-to-year variations were observed in melt onset (Figure 6). December was the month of maximum observed melt over the continent.

Peninsular shelves had minimum melt during 2013–14, whereas the melt over Amery shelf was maximum during the same period. The entire continent experienced its warmest summer during 2004–05 and coldest summer during 2011–12. Non-significant negative trend in MI and positive trend in MA were observed during the study period. Austral temperatures also showed negative trend over Amery and Larsen shalves.

A nonlinear regression was observed between austral mean monthly temperature and MI with correlation being 0.72 and 0.68 over Amery and Larsen shelves. High correlation between satellite-derived melt days and PDD (Figure 10) indicates effectiveness of the melt algorithm used, which can be utilized as a parameter to generate spatial duration map using satellite-based PDD data. MI was found to be negatively correrelated with December SAM index, indicating possibility of linkage between global climate and melt. Since the results were not significant, detailed analysis over the continent is needed before deriving further conclusion.

Surface melting is a variable phenomenon and fluctuations are observed over year to year and place to place. Melt surface area is important to monitor for large shelves. Oceansat data in continuation with QuikSCAT data had mapped MI over the entire continent with detailed results presented for 16 major shelves all along the Antarctic coast in different regions. Apart from known facts about more melt over West Antarctica, East Antarctica shelves also need constant monitoring for change in melt area and duration of melt. For a better understanding of temperature impact on the melt, it is proposed to use high-resolution satellite based temperature data.

1. Wen, J., Wang, Y., Wang, W., Jezek, K. C., Liu, H. and Allison, I., Basal melting and freezing under the Amery Ice Shelf, East Antarctica. *J. Glaciol.*, 2010, **56**, 195.
2. Scambos, T. *et al.*, Ice shelf disintegration by plate bending and hydro-fracture: satellite observations and model results of the 2008 Wilkins ice shelf break-ups. *Earth Planet. Sci. Lett.*, 2009, **280**, 51–60.
3. Trusel, L. D, Frey, K. E. and Das, S. B., Antarctic surface melting dynamics: enhanced perspectives from radar scatterometer data. *J. Geophys.*, 2012, **117**, F02023; doi: 10.1029/2011JF002126.
4. Kunz, L. B. and Long, D., Melt detection in Antarctic ice-shelves using scatterometers and microwave radiometers. *IEEE Trans. Geosci. Remote Sensing*, 2006, **44**, 2461–2469.
5. Liu, H., Wang, L. and Jezek, K. C., Spatiotemporal variations of snowmelt in Antarctica derived from satellite scanning multichannel microwave radiometer and Special Sensor Microwave Imager data (1978–2004). *J. Geophys. Res.*, 2006, **111**, F01003; doi: 10.1029/2005JF000318.
6. Barrand, N. E., Vaughan, D. G., Steiner, N., Tedesco, M., Kuipers Munneke, P., Van den Broeke, M. R. and Hosking, J. S., Trends in Antarctic Peninsula surface melting conditions from observations and regional climate modeling. *J. Geophys. Res.: Earth Surf.*, 2013, **118**, doi: 10.1029/2012JF002559.
7. Munneke, K., Picard, P. G., van den Broeke, M. R., Lenaerts, J. T. M. and van Meijgaard, E., Insignificant change in Antarctic snowmelt volume since 1979. *Geophys. Res. Lett.*, 2012, **39**, L01501; doi:10.1029/2011GL050207.
8. Zwally, H. J. and Fiegles, S., Extent and duration of Antarctic surface melting. *J. Glaciol.*, 1994, **40**, 136, 463–476.
9. Torinesi, O., Fily, M. and Genthon, C., Interannual variability and trend of the Antarctic summer melting period from 20 years of space-borne microwave data. *J. Climate*, 2003, **16**, 1047–1060.
10. Tedesco, M., Abdalati, W. and Zwally, H. J., Persistent surface snowmelt over Antarctica 1987–2006 from 19.35 GHz brightness temperatures. *Geophys. Res. Lett.*, 2007, **34**, L18504; doi: 10.1029/2007GL031199.
11. Markus, T., Stroeve, J. C. and Miller, J., Recent changes in Arctic sea ice melt onset, freeze-up, and melt season length. *J. Geophys. Res.*, 2009, **114**, C07005; doi: 10.1029/2009JC005436.
12. Stroeve, J. C., Markus, T., Boisvert, L., Miller, J. and Barrett, A., Changes in Arctic melt season and implications for sea ice loss. *Geophys. Res. Lett.*, 2014, **41**; doi: 10.1002/2013GL058951.
13. Hillard, U., Sridhar, V., Lettenmaier, D. P. and McDonald, K. C., Assessing snowmelt dynamics with NASA scatterometer NSCAT data and a hydrologic process model. *Remote Sensing Environ.*, 2003, **86**, 52–69; doi: 10.1016/S0034-42570300068-3.
14. Haarpaintner, J., Tonboe, R. T., Long, D. G. and VanWoert, M. L., Automatic detection and validity of sea ice edge: an application of enhanced resolution QuikScat/SeaWinds data. *IEEE Trans. Geosci. Remote Sensing Sci.*, 2004, **42**(7), 1433–1444.
15. Ojha, S. R., Singh, R. K., Vyas, K. N. and Sarkar, A., Study of inter-annual variations in surface melting over Amery Ice Shelf, East Antarctica, using space-borne scatterometer data. *J. Earth Syst. Sci.*, 2011, **120**(2), 329–336.
16. Dupont, F. *et al.*, Monitoring the melt season length of the Barnes Ice Cap over the 1979–2010 period using active and passive microwave remote sensing data. *Hydrol. Process.*, 2012, **26**(17), 2643–2652.

17. Oza, S. R., Spatial-temporal patterns of surface melting observed over Antarctic ice shelves using scatterometer data. *Antarct. Sci.*, 2015, 1–8; doi: 10.1017/S0954102014000832.
18. Bothale, R., Rao, P. V. N., Dutt, C. B. S. and Dadhwal, V. K., Detection of snowmelt and freezing in Himalaya using OSCAT data. *J. Earth Syst. Sci*., 2015, **124**(1), 101–113.
19. Sharp, M. and Wang, L., A five-year record of summer melt on Eurasian Arctic ice caps. *J. Climate*, 2009, **22**, 133–145.
20. Steiner, N. and Tedesco, M., A wavelet melt detection algorithm applied to enhanced-resolution scatterometer data over Antarctica 2000–2009. *Cryosphere*, 2014, **8**, 25–40; doi:10.5194/tc-8-25-2014.
21. Stiles, W. H. and Ulaby, F. T., The active and passive microwave response to snow parameters: part-1 – wetness; part 2 – water equivalent of dry snow. *J. Geophys. Res.*, 1980, **85**(2), 1037–1049.
22. Fung, A. K., *Microwave Scattering and Emission Models and their Applications*, Artech House, Norwood, 1994, p. 592.
23. Ulaby, F. T. and Long, D. G., *Microwave Radar and Radiometric Remote Sensing*, The University of Michigan Press, Ann Arbor, 2014, ISBN 978-0-472-11935-6.
24. Wismann, V., Monitoring of seasonal snowmelt on Greenland with ERS scatterometer data. *IEEE Trans. Geosci. Remote Sensing*, 2000, **38**, 1821–1826.
25. Wang, L., Sharp, M. J., Rivard, B., Marshall, S., Burgess, D. and Steffen, K., Melt season duration and ice layer formation on the Greenland ice sheet, 2000–2004. *J. Geophys. Res*., 2007, **112**, F04013; doi: 10.1029/2007JF000760.
26. Bhowmick, S. A., Kumar, R. and Kumar, A. S. K., Cross calibration of the OceanSAT-2 scatterometer with QuikSCAT scatterometer using natural terrestrial targets. *IEEE Trans. Geosci. Remote Sensing*, 2014, **52**, 3393–3398.
27. Finsterwalder, S. and Schunk, H., Der Suldenferner. *Z. Deulsclten Oseneich. Alpenvereills*, 1887, **18**, 72–89.
28. Nghiem, S. V. and Tsai, W. Y., Global snow cover monitoring with spaceborne Ku-band Scatterometer. *IEEE Trans. Geosci. Remote Sensing*, 2001, **39**, 10.
29. Bothale, R., Rao, P. V. N., Dutt, C. B. S. and Dadhwal, V. K., Dynamics of surface melting over Amery and Ross ice shelf in Antarctic using OSCAT data. In The International Archives of the Photogrammetry, Remote Sensing and Spatial Information Sciences, ISPRS Technical Commission VIII Symposium, 9–12 December 2014, Hyderabad, 2014, vol. XL-8; doi:10.5194/isprsarchives-XL-8-505-2014.
30. Picard, G., Fily, M. and Gallée, H., Surface melting derived from microwave radiometers: a climatic indicator in Antarctica, *Ann. Glaciol*., 2007, **46**, 29–34.
31. Tedesco, M. and Monaghan, A. J., An updated Antarctic melt record through 2009 and its linkages to high-latitude and tropical climate variability. *Geophys. Res. Lett*., 2009, **36**, L18502; doi: 10.1029/2009GL039186.
32. Marshall, G., Orr, A., Van Lipzig, N. and King, J., The impact of a changing southern hemisphere annular mode on Antarctic Peninsula summer temperatures. *J. Climate*, 2006, **19**, 5388–5404.

ACKNOWLEDGEMENTS. We thank the Australian Antarctic Division for providing temperature data for AWS stations and the AMRC, SSEC, UW-Madison for providing temperature data of UW AWS stations in Antarctica. The analysis has been done at the National Remote Sensing Centre, Hyderabad under the NICES programme. We also thank the three anonymous reviewers for critical comments which helped improve the manuscript.

Received 24 March 2015; revised accepted 8 May 2015